

Mechanistic insights into the early events in the aggregation of immunoglobulin light chains.

Pinaki Misra¹, Luis. M. Blancas-Mejia¹, Marina Ramirez-Alvarado^{1,2}.*

¹Department of Biochemistry and Molecular Biology and ²Department of Immunology, Mayo Clinic, Rochester, MN 55905, USA.

AL-Proteins	Low concentration	High Concentration
κ I O18/O8	23.2 \pm 0.2 μ M (n=3)	230.1 \pm 3.2 μ M (n=3)
AL-09	22.7 \pm 0.7 μ M (n=3)	220.3 \pm 12.6 μ M (n=3)
AL-09 H87Y	21.7 \pm 0.6 μ M (n=4)	207.6 \pm 2.8 μ M (n=2)
AL-12	22.8 \pm 1.1 μ M (n=5)	209.4 \pm 2.6 μ M (n=4)
AL-12 R65S	25.8 \pm 0.3 μ M (n=2)	216.3 \pm 1.8 μ M (n=3)

Table ST1: Actual concentration of AL proteins used in different experimental assays as determined by HPLC at Abs₂₈₀. “n” represents the number of biological replicates used to obtain the average concentration reported.

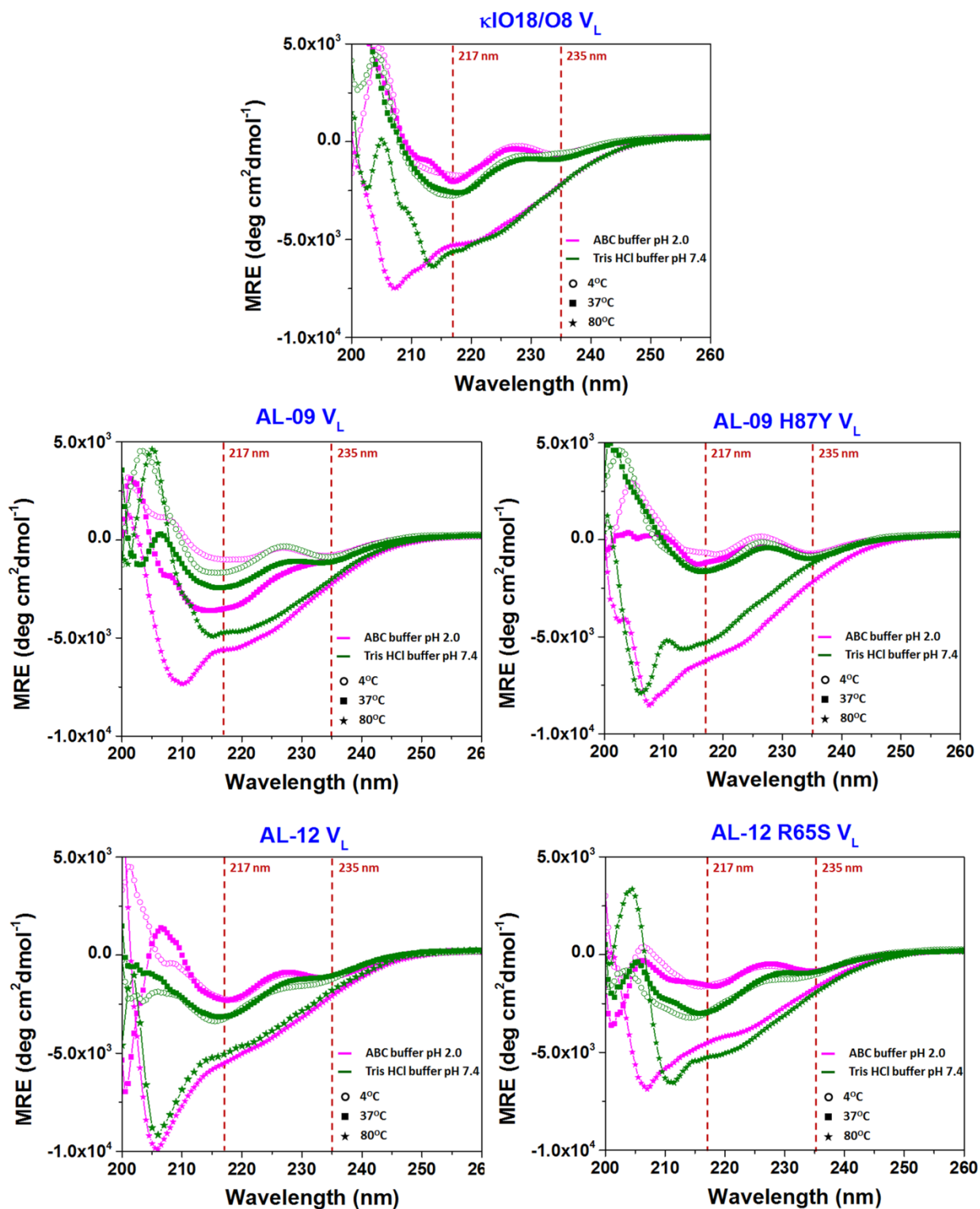


Figure S1: Comparative analysis of far UV-CD spectra of AL proteins. The far UV-CD spectra of the different AL-proteins in 10 mM ABC buffer pH 2.0 (magenta) and 10 mM Tris-

HCl buffer pH 7.4 (green) at 4°C (○), where all proteins are in the folded state, 37°C (■), where AL-09 is in the unfolding transition and 80°C (★), where all proteins are in the unfolded state.

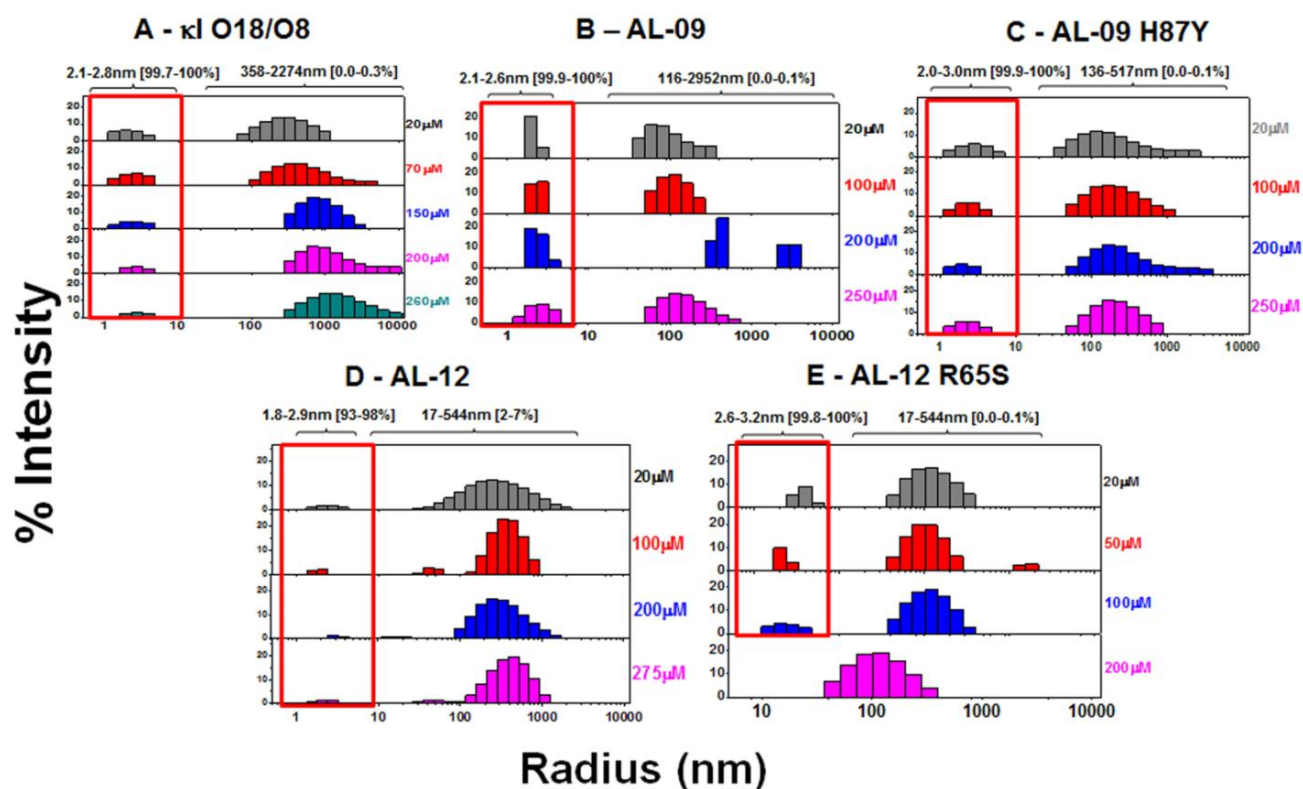


Figure S2: Size distribution analysis of monomeric particles in light chain variable domain proteins before experimental assay. Shown are peaks corresponding to hydrodynamic radii computed from scattering intensity in (A) κ I O18/O8, (B) AL-09, (C) AL-09 H87Y, (D) AL-12 and (E) AL-12 R65S at different concentrations in 10 mM Tris-HCl buffer at pH 7.4. The hydrodynamic radii (nm) of different population of particles represented by their respective peaks are mentioned above the graphs. Values presented in the parenthesis adjacent to hydrodynamic radii represent the population density in percent mass of the particles. The size

distribution ranging from 2.0-3.2 nm represents the predominant population (93-100%) of monomeric protein (represented under red squares) at each of the concentrations.

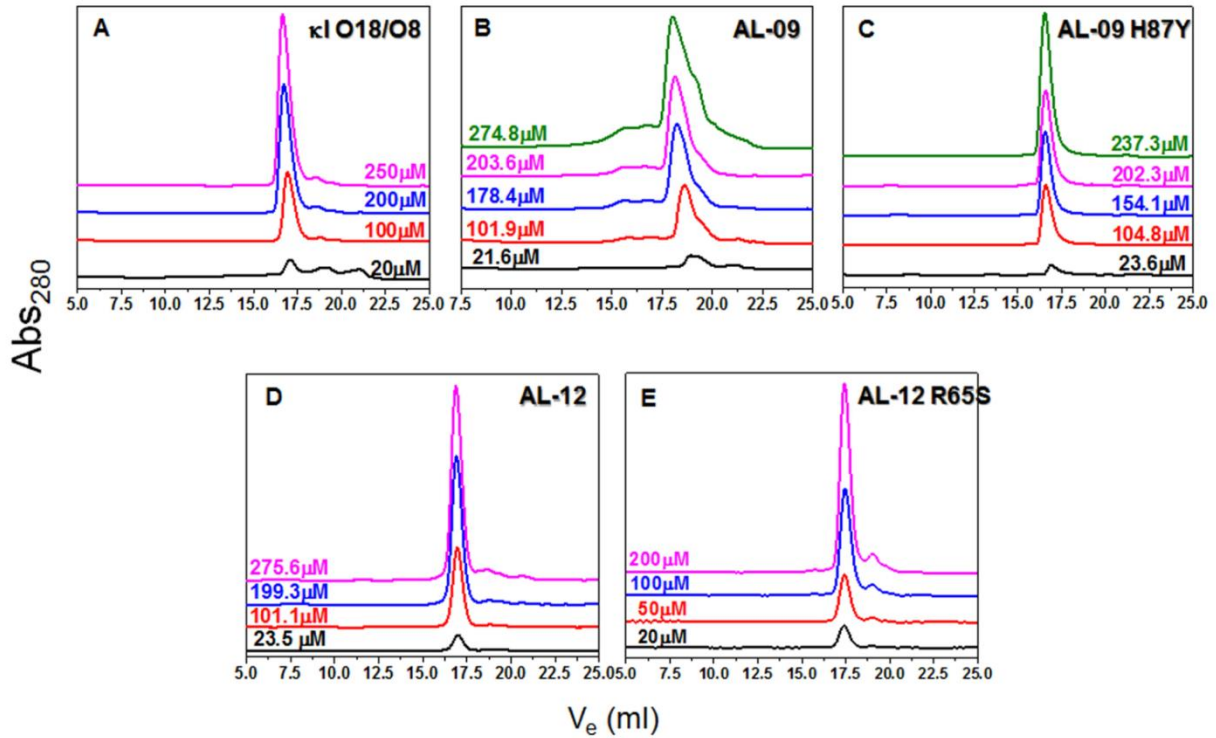


Figure S3: Determination of purity, homogeneity, and elution properties of monomeric state of light chain variable domain proteins before experimental assay. Shown are size exclusion chromatograms of light chain variable domain proteins (A) κI O18/O8, (B) AL-09, (C) AL-09 H87Y, (D) AL-12, and (E) AL-12 R65S at different concentrations prepared in 10 mM Tris-HCl buffer at pH 7.4.

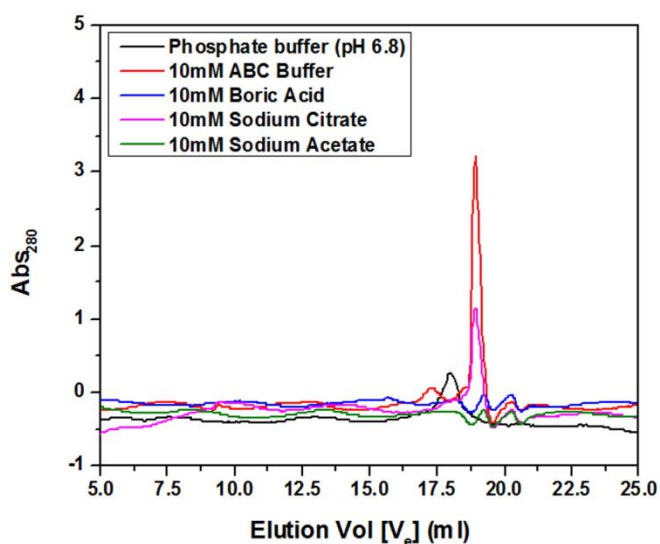


Figure S4: Investigation of baseline quality by analytical size exclusion chromatography prior to experimental assay. Chromatogram above shows baseline obtained in presence of different buffers and its constituents. 10 mM ABC buffer and its constituent 10 mM sodium citrate shows a significant absorbance ($A_{280\text{ nm}}$) at $V_e = 18.6\text{ mL}$.

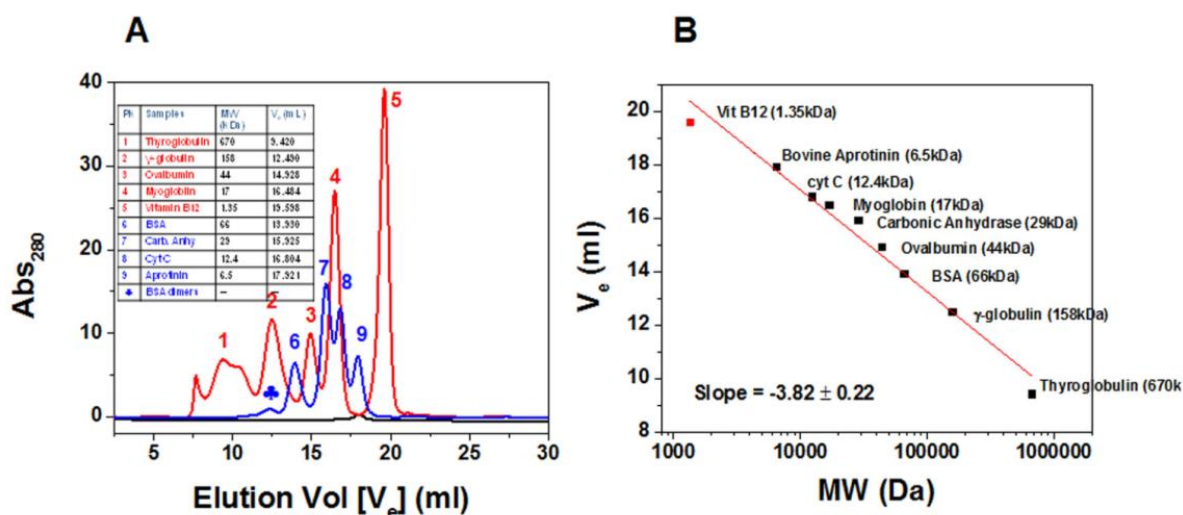


Figure S5: Protein standards injection in analytical size exclusion chromatography to determine the apparent molecular weight of unknown species during aggregation. (A) Shows elution volume (V_e) obtained from injecting different proteins with known molecular weights (MW). (B) Plot of V_e vs log MW of constituent proteins fitted to linear regression. Linear regression fitting parameters were used to determine the apparent molecular weight of the unknown species during aggregation.

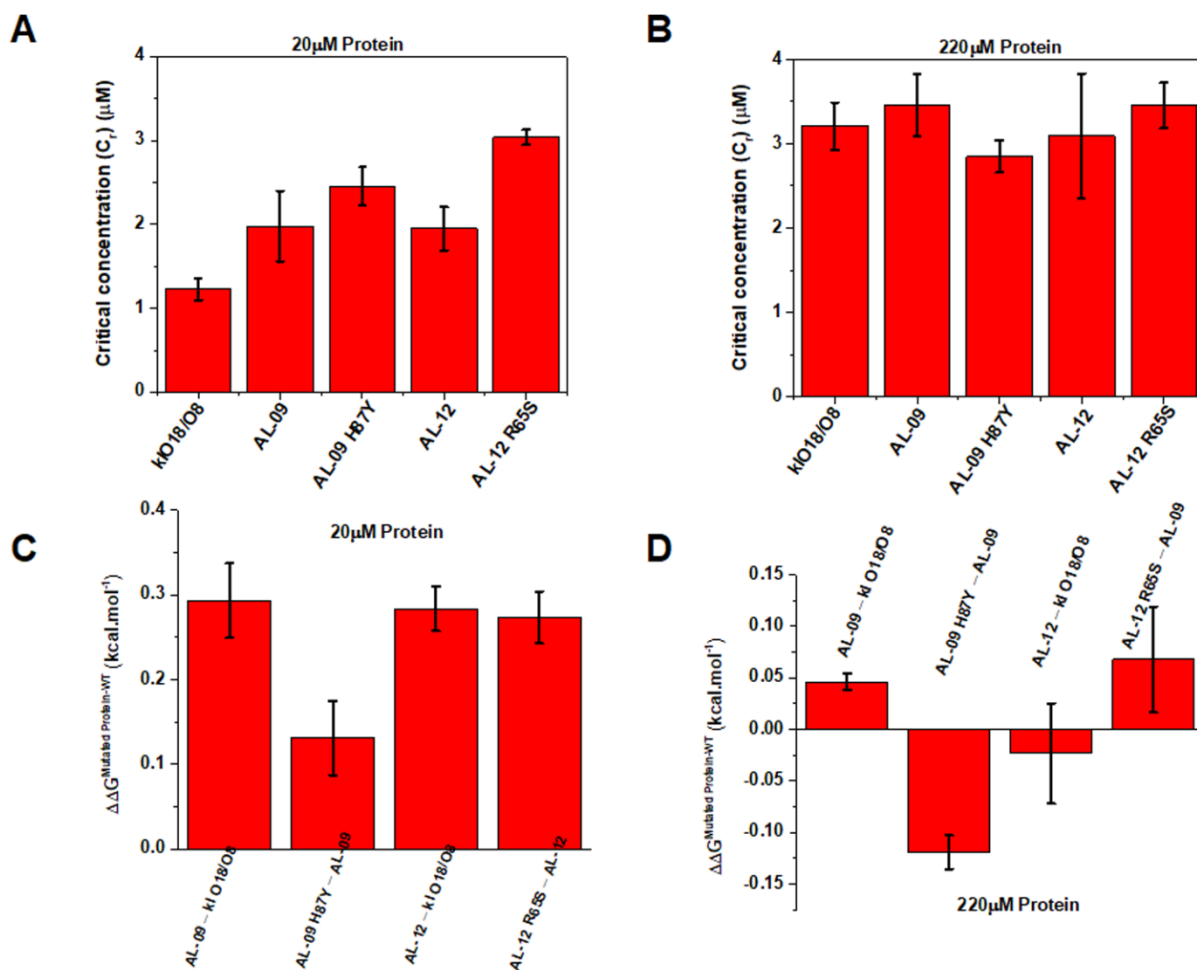


Figure S6: Critical concentration (C_r) and $\Delta\Delta G$ values of different light chain variable domain proteins. Shown are C_r of different light variable domain proteins at (A) 20 μ M and (B)

220 μM . $\Delta\Delta\text{G}$ ($\Delta\text{G}_{\text{Mutated Proteins}} - \Delta\text{G}_{\text{WT}}$) values at (C) 20 μM and (D) 220 μM . Aggregation mixture for all the above experiments were prepared in 10 mM ABC buffer at pH 2.0. *Error bars represent Standard error of mean.*

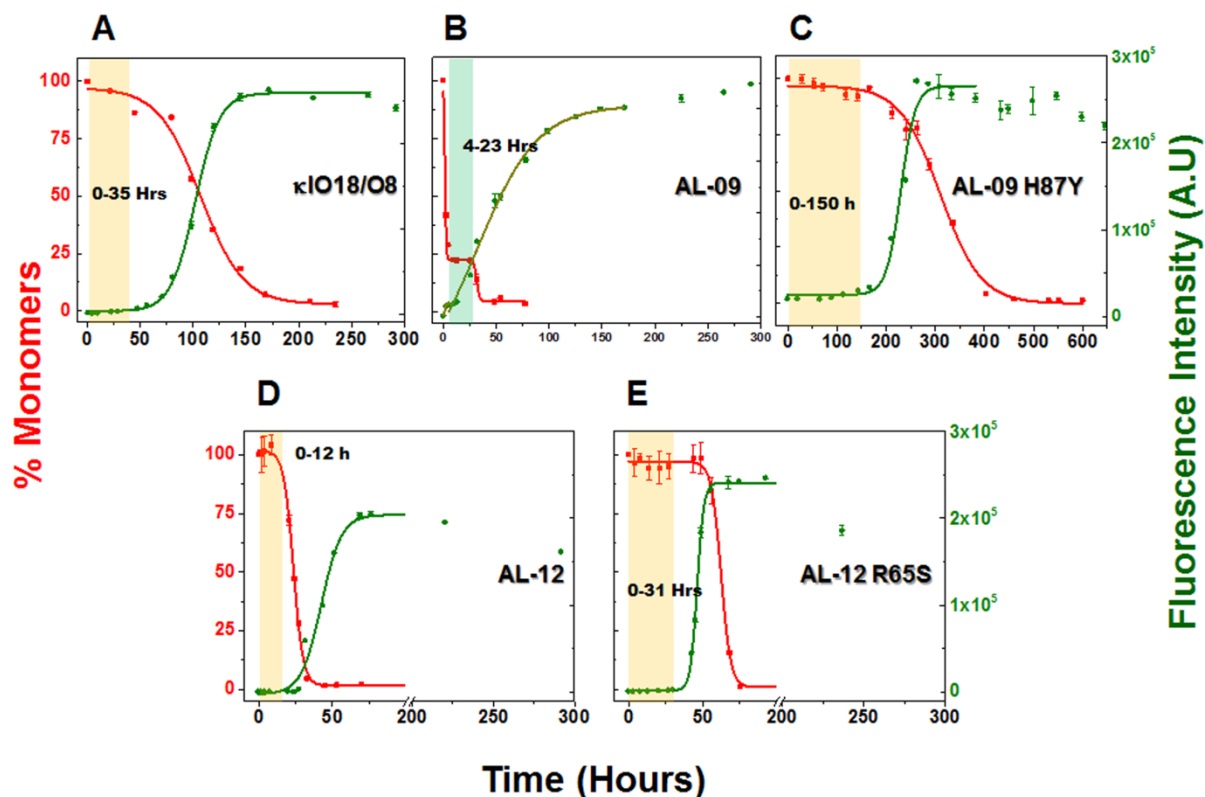


Figure S7: Comparative analysis of aggregation rate in different light chain variable domain proteins at 220 μM . Shown are the representative kinetic traces of different time points obtained from sedimentation assay to calculate the % monomer remaining in the reaction (■) vs ThT Assay (●) at 220 μM of (A) $\kappa\text{I O18/O8}$, (B) AL-09, (C) AL-09 H87Y, (D) AL-12, (E) AL-12 R65S. Kinetic traces at each time point are from duplicate readings. Aggregation mixture for all the above experiments were prepared in 10 mM ABC buffer at pH 2.0. The highlighted area

in salmon in the graphs represents the nucleation phase presumed for this study (based on % monomer data). The highlighted area in green in the AL-09 graph represents a stable plateau phase during which the concentration of monomers remains unchanged. *Error bars represent Standard error of mean.*

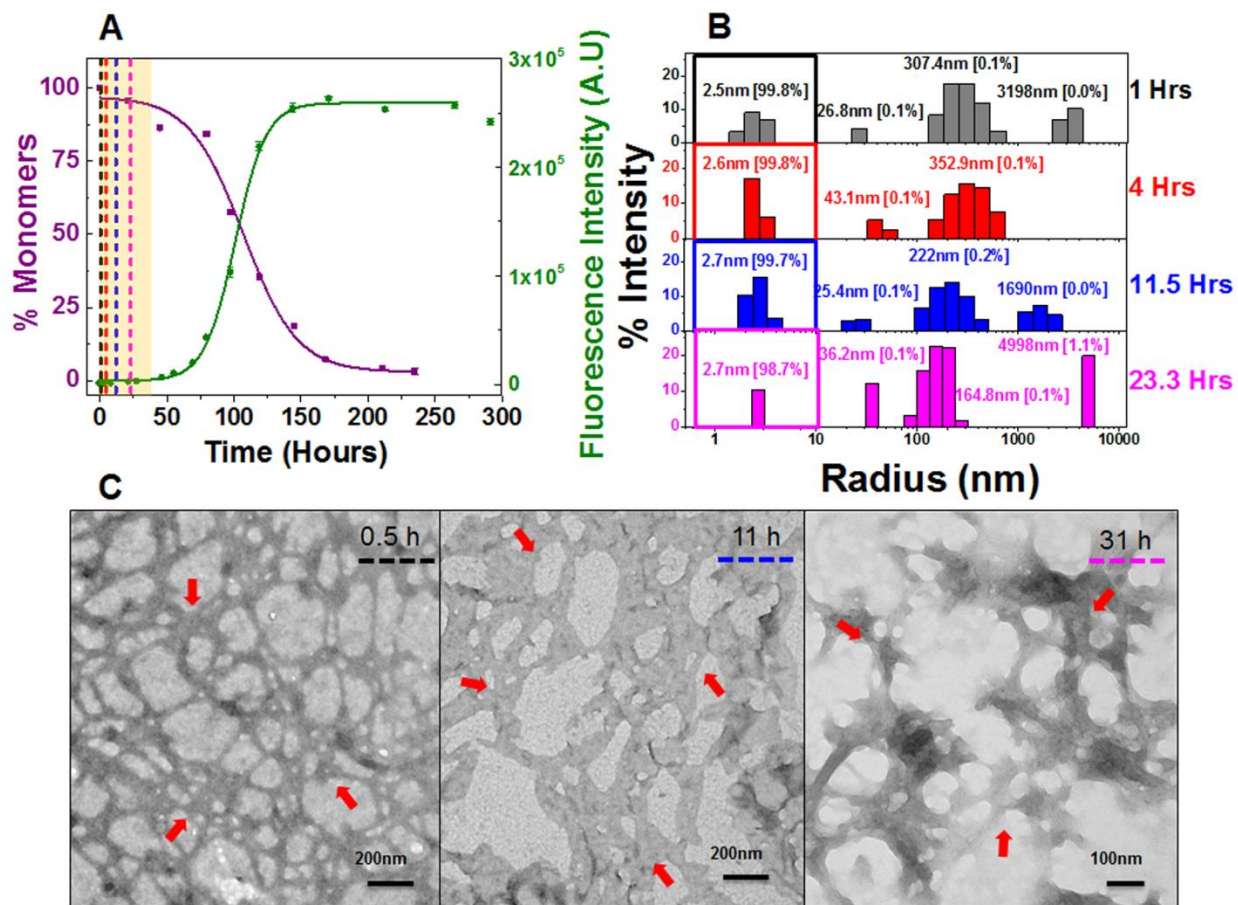


Figure S8: Composite analysis of monomer concentration, species size and abundance, and morphologies at 220 μ M κ I O18/O8 during nucleation. Shown are (A) the representative kinetic traces of the sedimentation (■) vs ThT Assay (●). The highlighted area in salmon represents the nucleation phase (based on % monomer data). The color coded dotted lines in (A)

represents the time points when DLS was performed. (B) Peaks corresponding to hydrodynamic radii computed from scattering intensity obtained from DLS. The peaks inside the colored squares represent the radius corresponding to the monomeric protein. Values presented in the parenthesis adjacent to hydrodynamic radii represent the population density in percent mass of particles. (C) Electron Micrographs of 220 μ M κ I O18/O8 at different time points during the course of aggregation. The color matched dotted line in the EM images compared to (A) and (B) represents the closest time points when aliquots from the reaction mixture were studied during the course of aggregation. Arrow designation: (\rightarrow) Aggregated nebular mesh of non-fibrillar oligomers. *Scale bar*, 100nm. Aggregation conditions: 10 mM ABC buffer at pH 2.0, 37°C, 300 rpm. *Error bars in (A) represent Standard error of mean.*

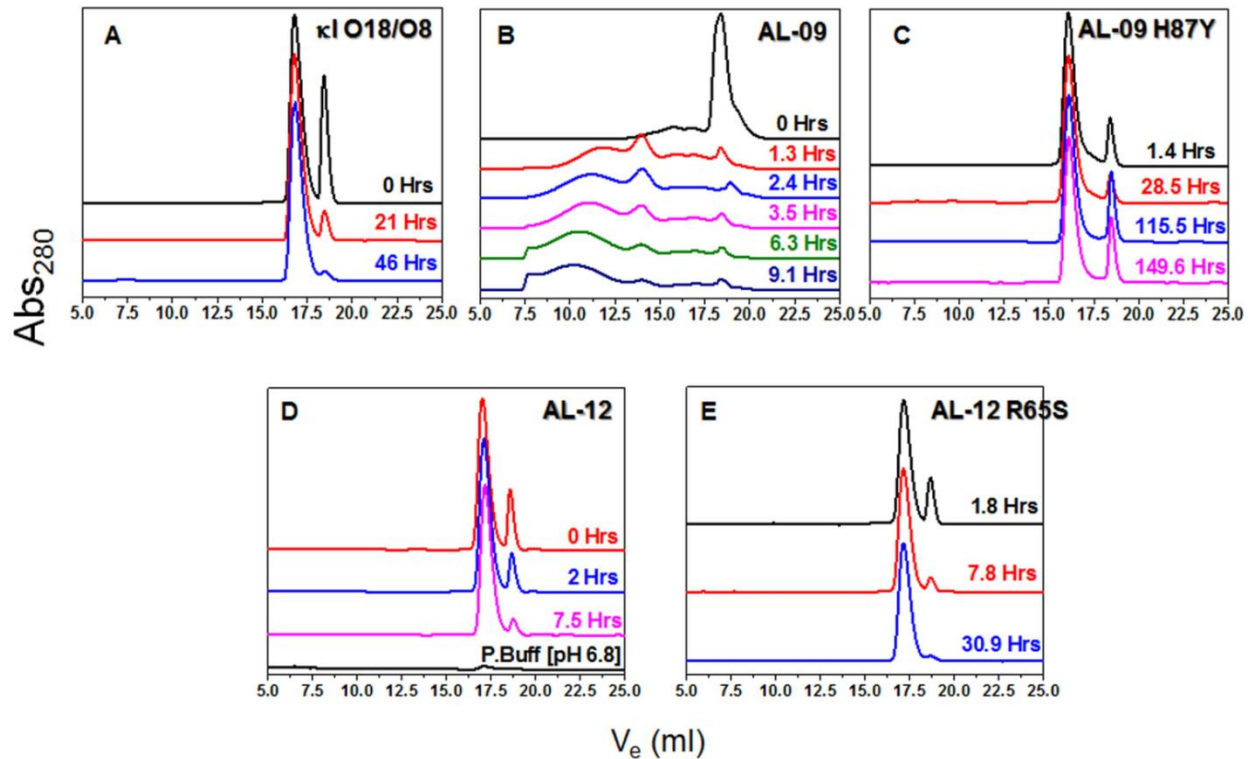


Figure S9: Elution properties of different species observed during the course of aggregation in light chain variable domain proteins. Size exclusion chromatograms of 220 μM of (A) κI O18/O8, (B) AL-09, (C) AL-09 H87Y, (D) AL-12, (E) AL-12 R65S at different time points, prepared in 10 mM ABC buffer at pH 2.0. The peak at $V_e \sim 18.6$ mL originates from absorption by sodium citrate in ABC buffer at 280 nm (for details see Figure S4)

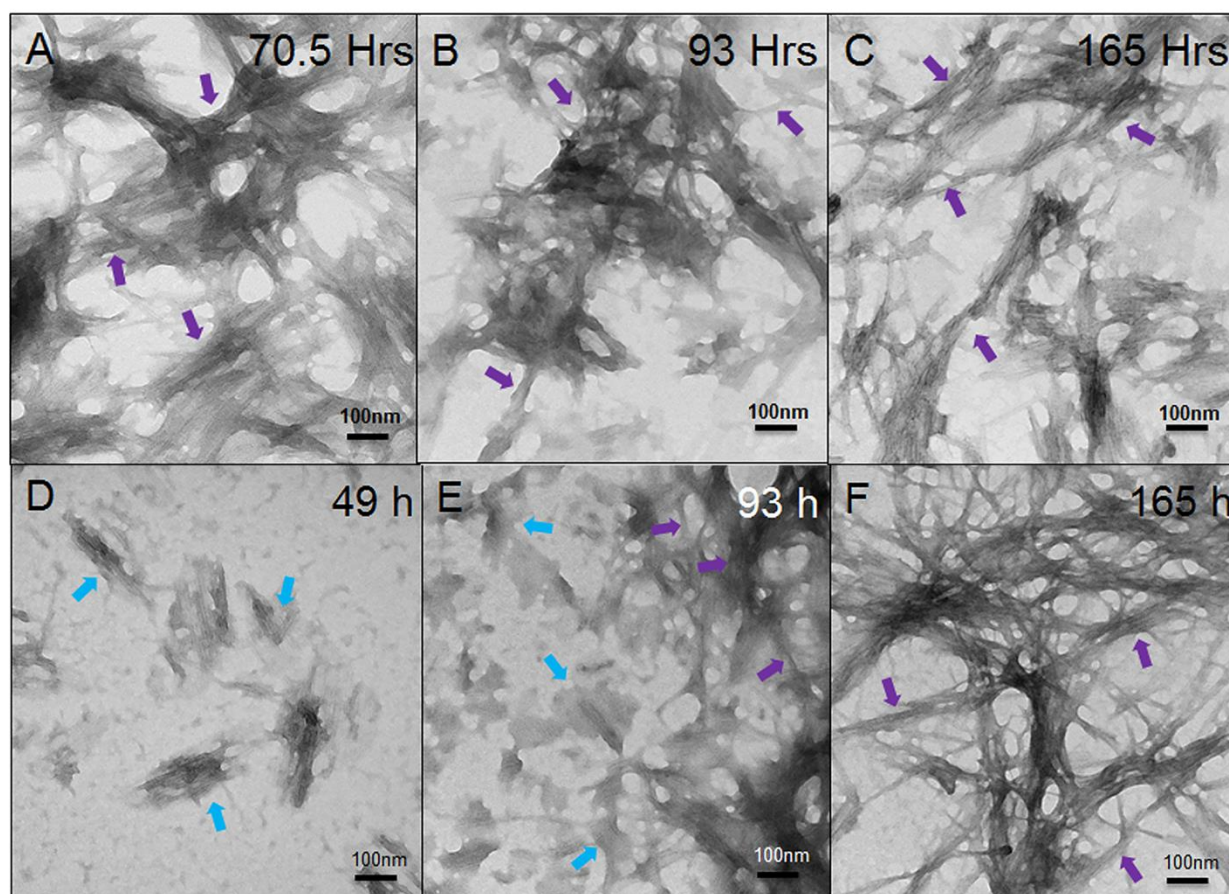


Figure S10: Electron Micrographs of κI O18/O8 at different time points after nucleation phase (10 mM ABC buffer, pH 2.0) at 20 μM (A-C) and 220 μM (D-F). Arrow designation: (→) Bundles of short fibrils (→) clusters of mature long fibrils. *Scale bar*, 100nm.

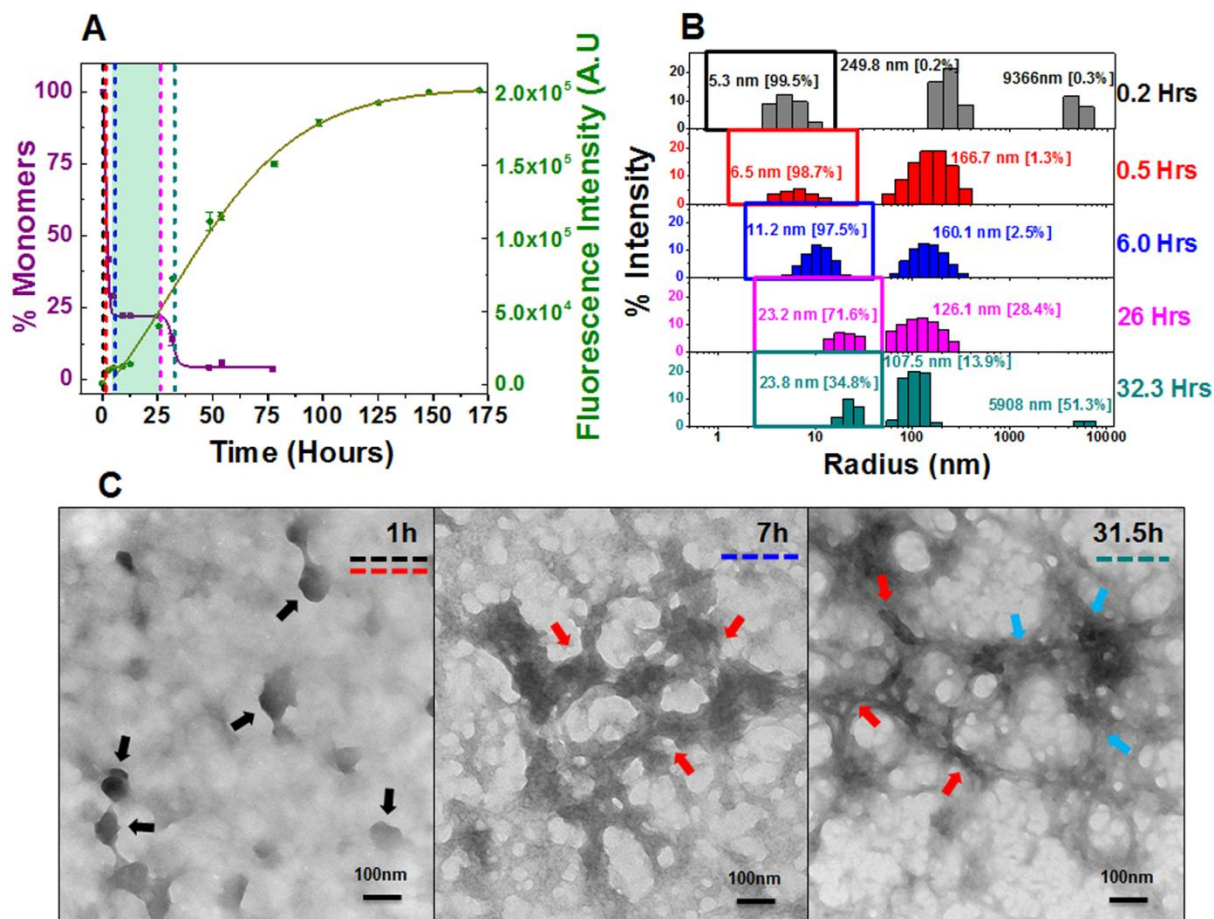


Figure S11: Composite analysis of monomer concentration, species size and abundance, and aggregate morphologies for 220 μ M AL-09 during nucleation phase. Shown are (A) the representative kinetic traces of the sedimentation assay to calculate the % monomer remaining in the reaction (■) vs ThT Assay (●). The highlighted area in green represents the plateau phase of the reaction (based on constant % monomeric concentration). The color coded dotted lines in (A) represents the time points when DLS was performed. (B) Peaks corresponding to hydrodynamic radii computed from scattering intensity obtained from DLS. The peaks inside the colored squares represent the radius corresponding to the intermediates. Values presented in the parenthesis adjacent to hydrodynamic radii represent the population density in percent mass of

particles. (C) Electron Micrographs of 220 μM AL-09 at different time points during the course of aggregation. The color matched dotted line in the EM images compared to (A) and (B) represents the closest time points when aliquots from the reaction mixture were studied during the course of aggregation. Arrow designation: (\rightarrow) Spherical oligomers, (\rightarrow) Aggregated nebular mesh of non-fibrillar oligomers, (\rightarrow) Bundles of short fibrils. *Scale bar*, 100nm. Aggregation conditions: 10 mM ABC buffer at pH 2.0, 37°C, 300 rpm. *Error bars in (A) represent Standard error of mean.*

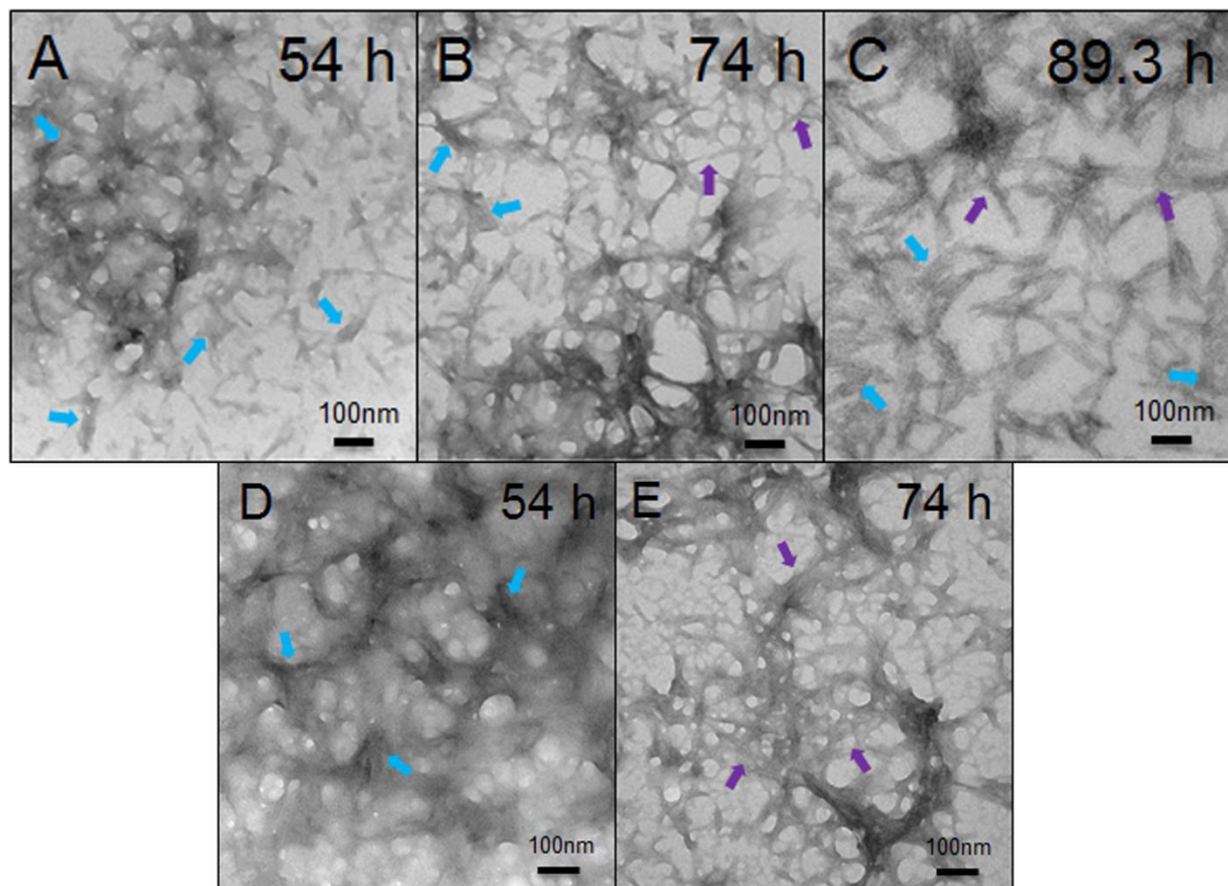


Figure S12: Electron Micrographs of AL-09 at different time points after nucleation phase (10 mM ABC buffer, pH 2.0) at 20 μ M (A-C) and 220 μ M (D,E). Arrow designation: (\rightarrow) Bundles of short fibrils (\rightarrow) clusters of mature long fibrils. Scale bar, 100nm.

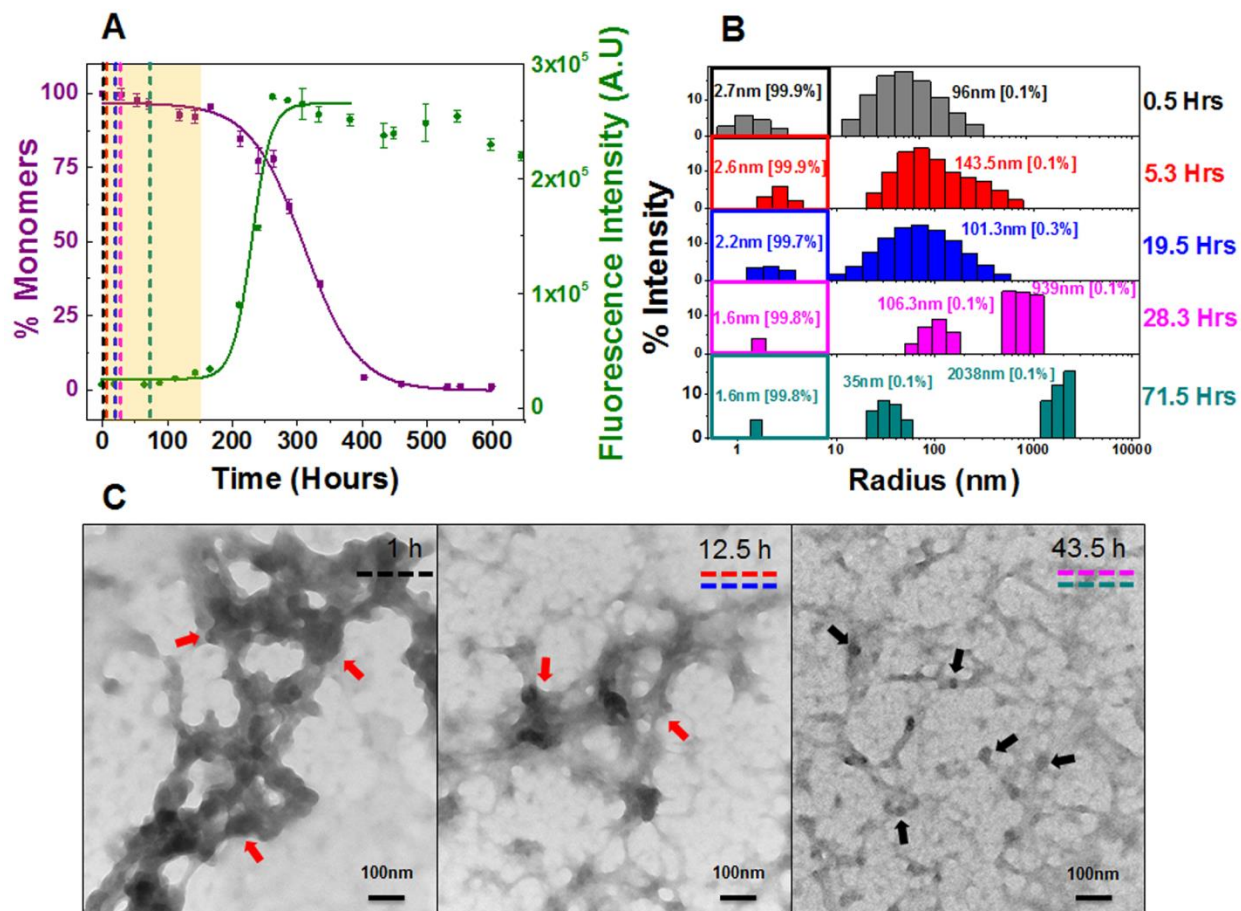


Figure S13: Composite analysis of monomer concentration, species size and abundance, and morphologies at 220 μ M AL-09 H87Y during nucleation. Shown are (A) the representative kinetic traces of the sedimentation assay (\blacksquare) vs ThT Assay (\bullet). The highlighted area in salmon represents the nucleation phase (based on % monomer data). The color coded dotted lines in (A) represents the time points when DLS was performed. (B) Peaks corresponding

to hydrodynamic radii computed from scattering intensity obtained from DLS. The peaks inside the colored squares represent the radius corresponding to the monomeric protein. Values presented in the parenthesis adjacent to hydrodynamic radii represent the population density in percent mass of particles. (C) Electron Micrographs of 220 μM AL-09 H87Y at different time points during the course of aggregation. The color matched dotted line in the EM images compared to (A) and (B) represents the closest time points when aliquots from the reaction mixture were studied during the course of aggregation. Arrow designation: (\rightarrow) Spherical oligomers, (\rightarrow) Aggregated nebular mesh of non-fibrillar oligomers. *Scale bar*, 100nm. Aggregation conditions: 10 mM ABC buffer at pH 2.0, 37°C, 300 rpm. *Error bars in (A) represent Standard error of mean.*

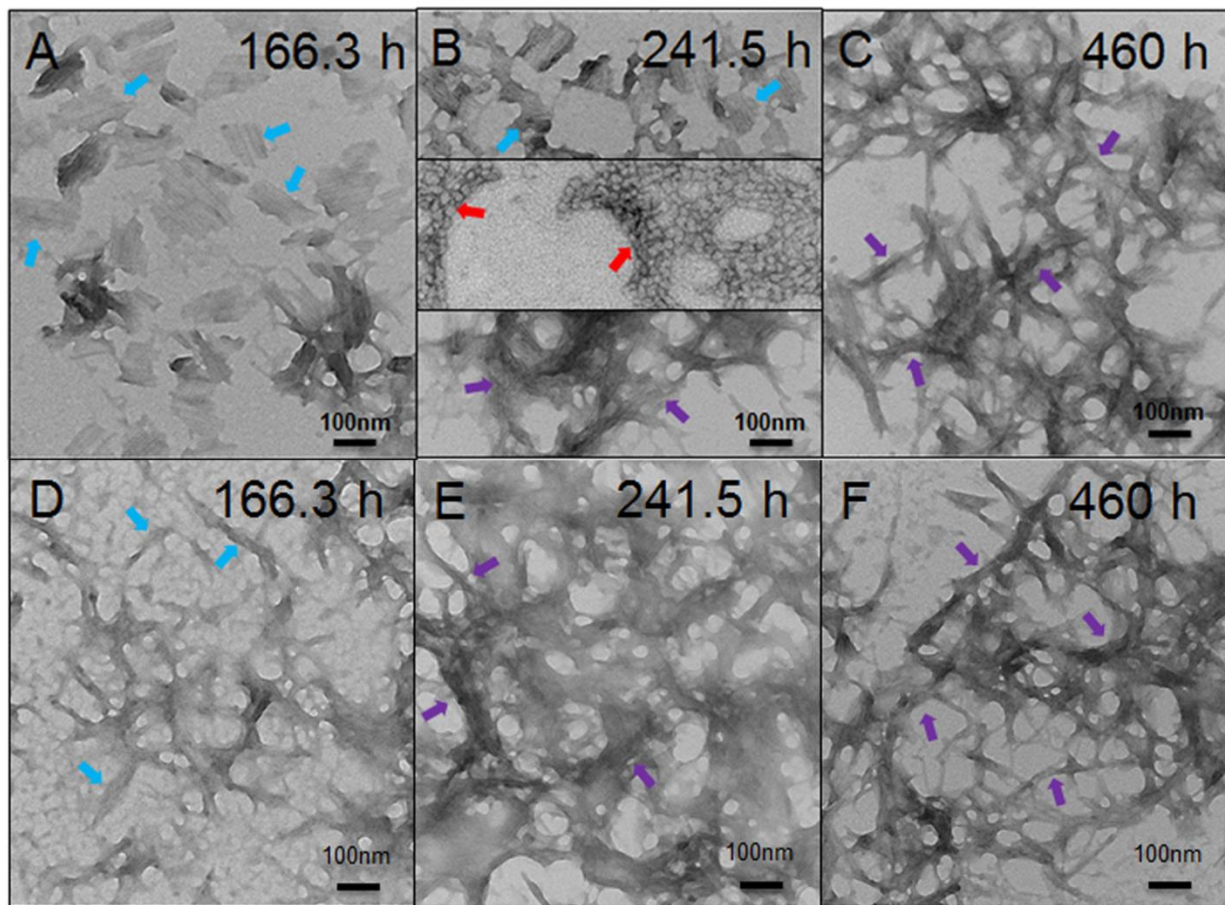


Figure S14: Electron Micrographs of AL-09 H87Y at different time points after nucleation phase (10 mM ABC buffer, pH 2.0) at 20 μ M (A-C) and 220 μ M (D-F). We included multiple images where there were more than one dominant species present in the time point samples. Arrow designation: (→) Aggregated nebular mesh of non-fibrillar oligomers, (↗) Bundles of short fibrils (↘) clusters of mature long fibrils. Scale bar, 100nm.

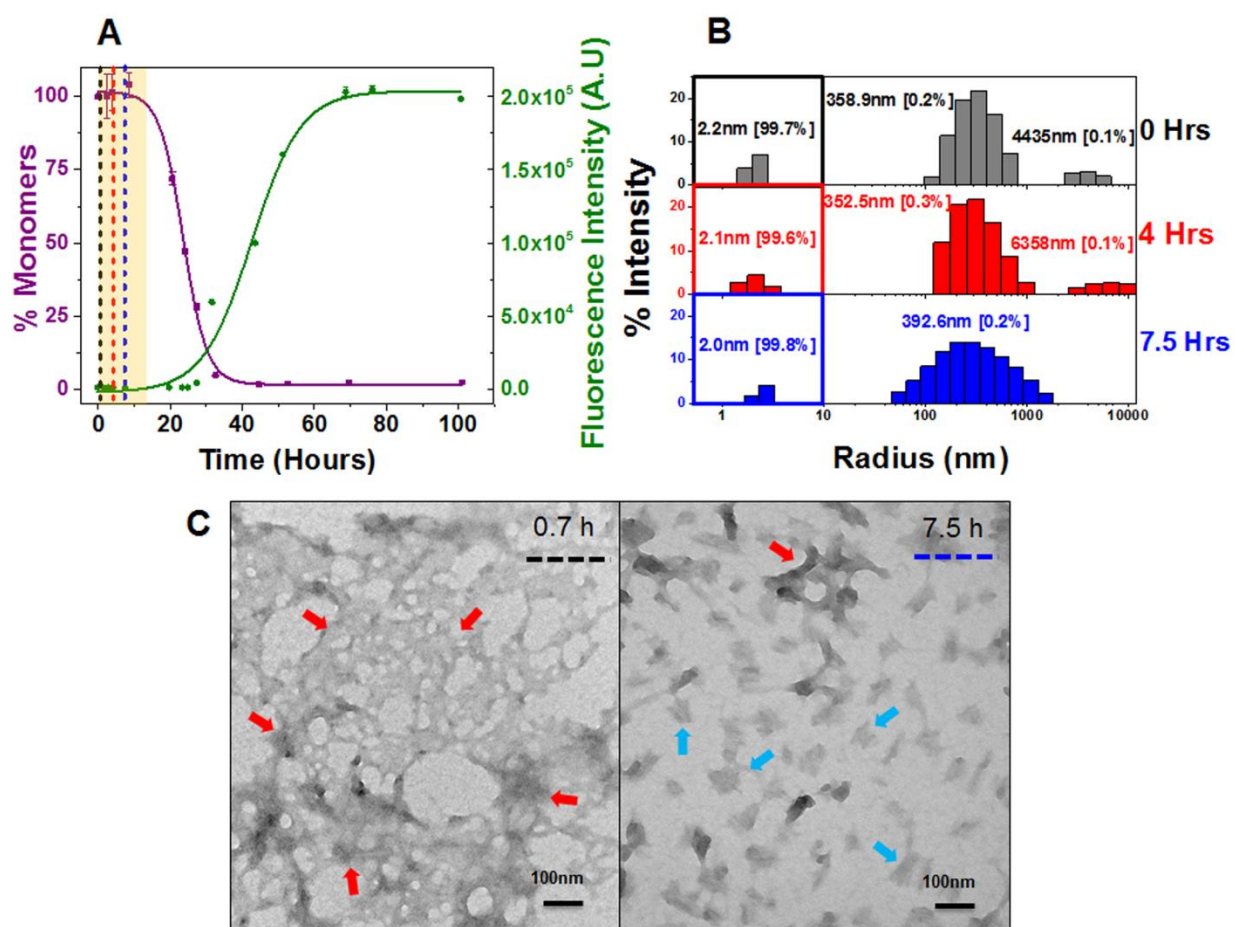


Figure S15: Composite analysis of monomer concentration, species size and abundance, and morphologies at 220 μ M AL-12 during nucleation. Shown are (A) the representative kinetic traces of the sedimentation assay (■) vs ThT Assay (●). The highlighted area in salmon

represents the nucleation phase (based on % monomer data). The color coded dotted lines in (A) represents the time points when DLS was performed. (B) Peaks corresponding to hydrodynamic radii computed from scattering intensity obtained from DLS. The peaks inside the colored squares represent the radius corresponding to the monomeric protein. Values presented in the parenthesis adjacent to hydrodynamic radii represent the population density in percent mass of particles. (C) Electron Micrographs of 220 μ M AL-12 at different time points during the course of aggregation. The color matched dotted line in the EM images compared to (A) and (B) represents the closest time points when aliquots from the reaction mixture were studied during the course of aggregation. Arrow designation: (→) Aggregated nebular mesh of non-fibrillar oligomers, (→) Bundles of short fibrils. *Scale bar*, 100nm. Aggregation conditions: 10 mM ABC buffer at pH 2.0, 37°C, 300 rpm. *Error bars in (A) represent Standard error of mean.*

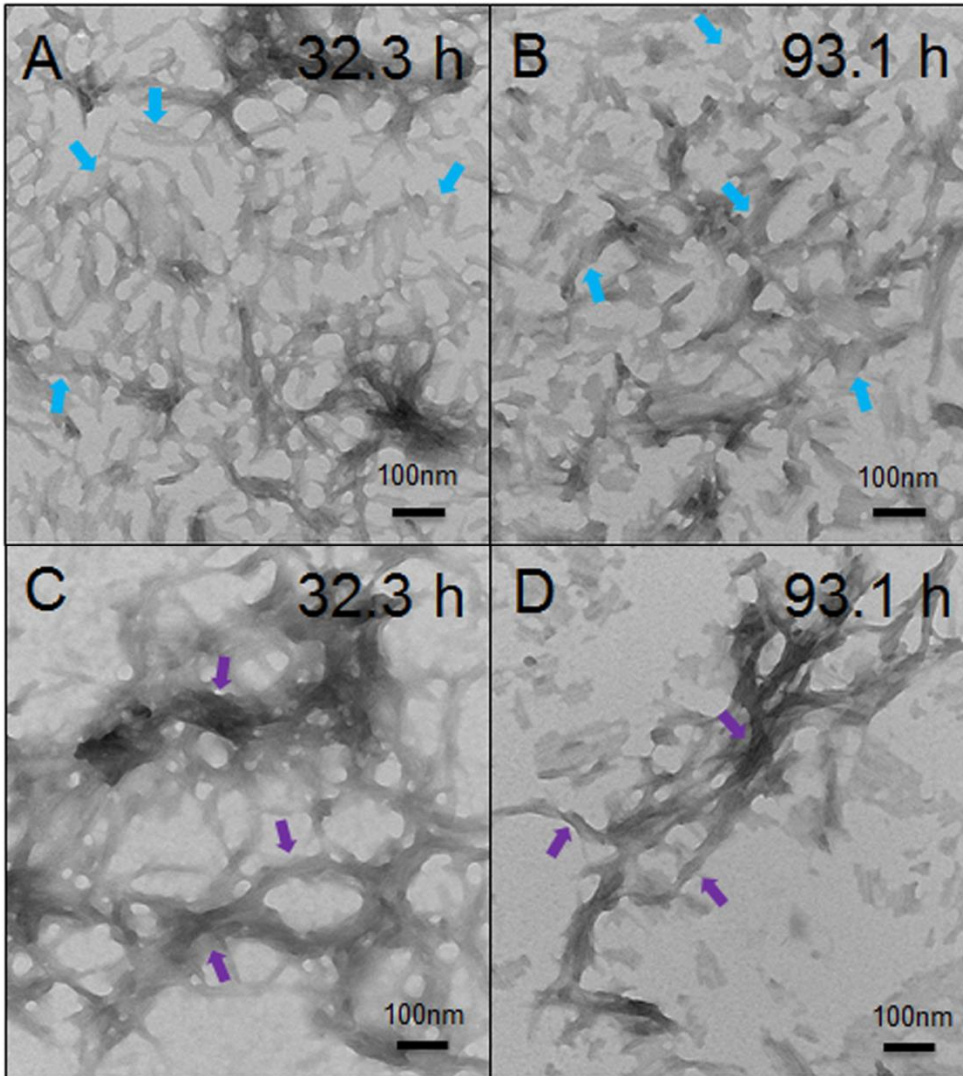


Figure S16: Electron Micrographs of AL-12 at different time points after nucleation phase (10 mM ABC buffer, pH 2.0) at 20 μ M (A,B) and 220 μ M (C,D). Arrow designation: (→) Bundles of short fibrils (→) clusters of mature long fibrils. *Scale bar*, 100nm.

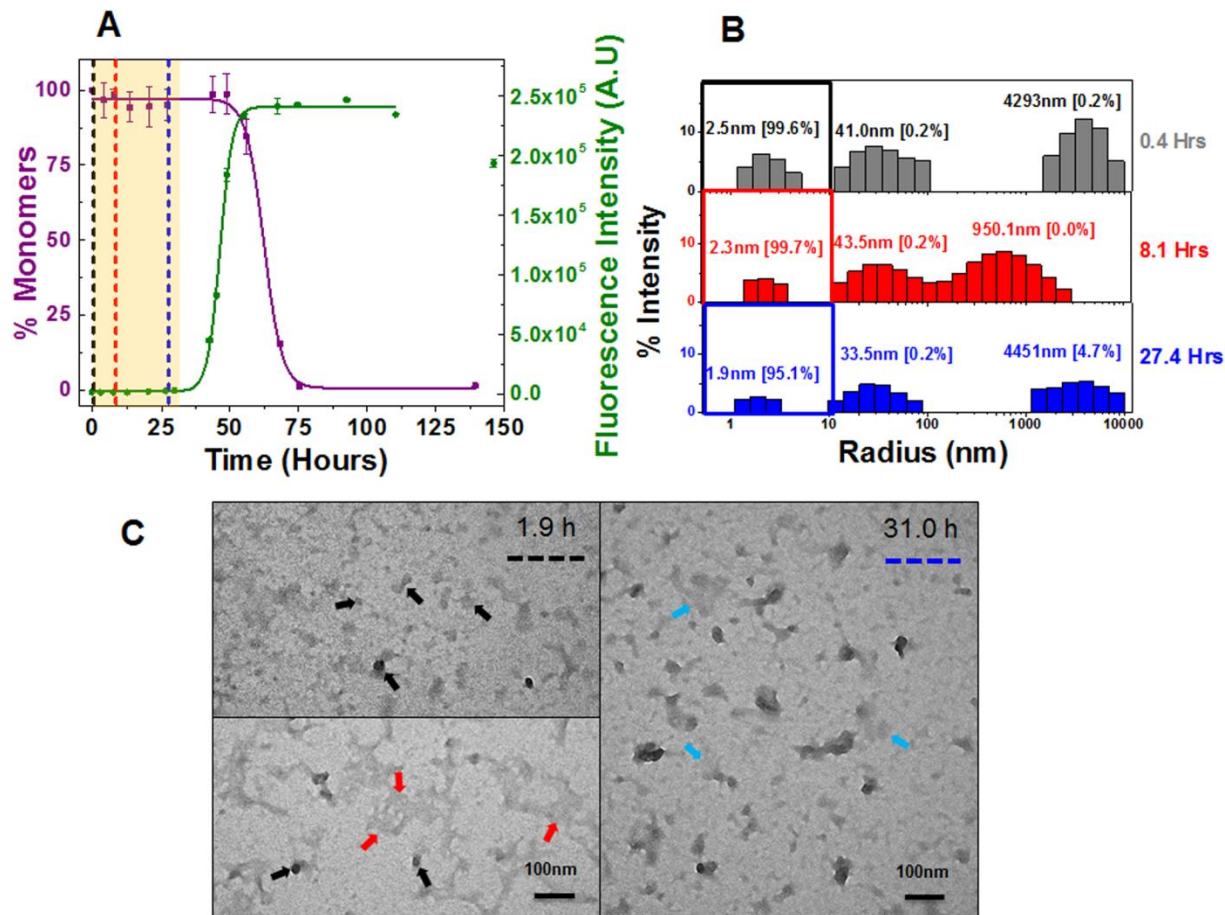


Figure S17: Composite analysis of monomer concentration, species size and abundance, and morphologies at 220 μ M AL-12 R65S during nucleation. Shown are (A) the representative kinetic traces of the sedimentation assay (\blacksquare) vs ThT Assay (\bullet). The highlighted area in salmon represents the nucleation phase (based on % monomer data). The color coded dotted lines in (A) represents the time points when DLS was performed. (B) Peaks corresponding to hydrodynamic radii computed from scattering intensity obtained from DLS. The peaks inside the colored squares represent the radius corresponding to the monomeric protein. Values presented in the parenthesis adjacent to hydrodynamic radii represent the population density in percent mass of particles. (C) Electron Micrographs of 220 μ M AL-12 R65S at different time points during the course of aggregation. The color matched dotted line in the EM images

compared to (A) and (B) represents the closest time points when aliquots from the reaction mixture were studied during the course of aggregation. Arrow designation: (→) Spherical oligomers, (→) Aggregated nebular mesh of non-fibrillar oligomers, (→) Bundles of short fibrils. *Scale bar*, 100nm. Aggregation conditions: 10 mM ABC buffer at pH 2.0, 37°C, 300 rpm. *Error bars in (A) represent Standard error of mean.*

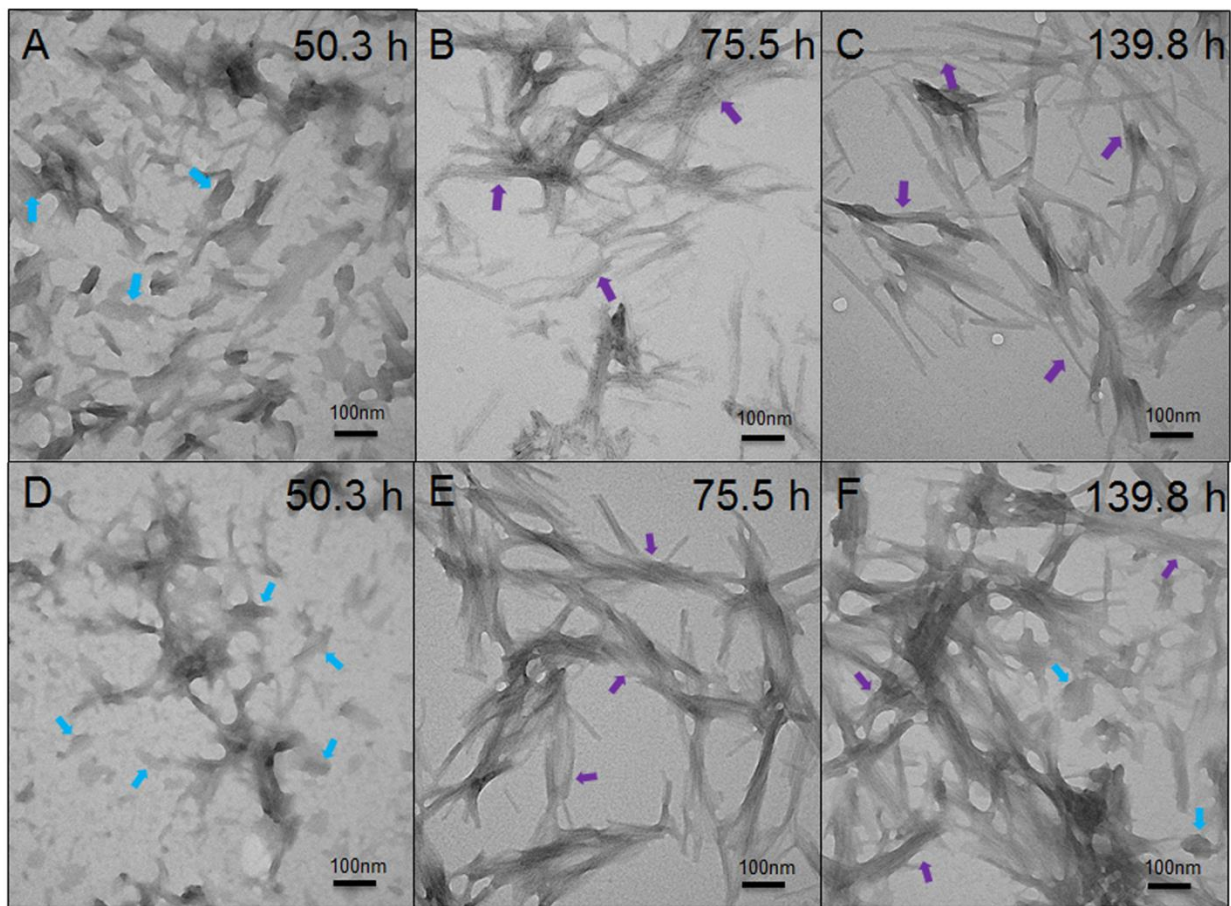


Figure S18: Electron Micrographs of AL-12 R65S at different time points after nucleation phase (10 mM ABC buffer, pH 2.0) at 20 μM (A-C) and 220 μM (D-F). Arrow designation: (→) Bundles of short fibrils (→) clusters of mature long fibrils. *Scale bar*, 100nm.